

Transport of the Lysosomal Membrane Glycoprotein lgp120 (lgp-A) to Lysosomes Does Not Require Appearance on the Plasma Membrane

Cordula Harter and Ira Mellman

Department of Cell Biology, Yale University School of Medicine, New Haven, Connecticut 06510

Abstract. We have used stably transfected CHO cell lines to characterize the pathway of intracellular transport of the lgp120 (lgp-A) to lysosomes. Using several surface labeling and internalization assays, our results suggest that lgp120 can reach its final destination with or without prior appearance on the plasma membrane. The extent to which lgp120 was transported via the cell surface was determined by two factors: expression level and the presence of a conserved glycine-tyrosine motif in the cytoplasmic tail. In cells expressing low levels of wild-type lgp120, the majority of newly synthesized molecules reached lysosomes without becoming accessible to antibody or biotinylation reagents added extracellularly at 4°C. With increased expression levels, however, an increased fraction of trans-

ported lgp120, as well as some endogenous lgp-B, appeared on the plasma membrane. The fraction of newly synthesized lgp120 reaching the cell surface was also increased by mutations affecting the cytoplasmic domain tyrosine or glycine residues. A substantial fraction of both mutants reached the surface even at low expression levels. However, only the lgp120G→A7 mutant was rapidly internalized and delivered from the plasma membrane to lysosomes. Taken together, our results show that the majority of newly synthesized wild-type lgp120 does not appear to pass through the cell surface en route to lysosomes. Instead, it is likely that lysosomal targeting involves a saturable intracellular sorting site whose affinity for lgp's is dependent on a glycine-tyrosine motif in the lgp120 cytoplasmic tail.

LYSOSOMES contain a characteristic set of highly glycosylated membrane proteins. By cloning cDNAs from different species (Cha et al., 1990; Chen et al., 1988; Fambrough et al., 1988; Granger et al., 1990; Himeno et al., 1989; Howe et al., 1988; Noguchi et al., 1989; Viitala et al., 1988), they have been divided in two groups (lgp-A and lgp-B) that share a high degree of homology in their overall structure and sequence (Kornfeld and Mellman, 1989). Features common to all lgp's include a large number of N-linked oligosaccharides in their luminal domain, a single transmembrane anchor, and a short 10–11-amino acid cytoplasmic tail. Despite their well-characterized biochemical properties, nothing is known about the functions of lgp's.

Another important but as yet unresolved issue concerns the pathways taken by lgp's from the Golgi complex to late endosomes and lysosomes. Transport to lysosomes might occur after the delivery of newly synthesized lgp's to the plasma membrane and subsequent endocytosis. Alternatively, lgp's might be sorted intracellularly and reach endosomes and/or lysosomes without appearing on the cell surface. Several considerations suggest that either or both possibilities may occur.

Kinetic studies of lgp120 (lgp-A) transport to lysosomes in normal rat kidney (NRK)¹ cells and mouse macrophages

suggested directed delivery of lgp's to lysosomes without initial transport to the plasma membrane (Green et al., 1987). This conclusion was based on the observation that lgp120 was transported from the Golgi complex to lysosomes as fast as plasma membrane proteins were transported from the Golgi complex to the cell surface; thus, the initial cohort of newly synthesized lgp molecules reached lysosomes too rapidly to have involved obligatory transport through the cell surface. A similar conclusion was reached by cell fractionation for mouse lamp-1 (lgp-A) in 3T3 cells (D'Souza and August, 1986). Conceivably, transport of lysosomal membrane components may follow the same pathway taken by newly synthesized lysosomal enzymes bound to the cation-independent mannose 6-phosphate receptor (MPR). In this case, several considerations indicate that enzyme-receptor complexes leave the *trans*-Golgi network (TGN) in clathrin-coated vesicles which deliver their contents to endosomes and, in turn, to lysosomes without reaching the cell surface (for review see Kornfeld and Mellman, 1989). A similar finding for lgp's would imply that these molecules too possess a sorting determinant that directs their transport upon exit from the TGN.

The alternative route, appearance on the cell surface followed by endocytosis, has been suggested to occur for at least a portion of the lgp molecules in chicken fibroblasts (LEP100, lgp-A; Lippincott-Schwartz and Fambrough, 1986), primary rat hepatocytes (LGP107, lgp-A; Furuno et al., 1989a,b), human leukemia cells (lamp-1, lgp-A; Mane et

¹ *Abbreviations used in this paper:* LAP, lysosomal acid phosphatase; MPR, mannose 6-phosphate receptor; NRK cells, normal rat kidney cells; TGN, *trans*-Golgi network.

al., 1989), and MDCK cells (AC17 antigen; Nabi et al., 1991). Based on antibody binding, each of these studies found 2–3% of total lgp on the cell surface at steady state and that anti-*lgp* antibody could be internalized at 37°C. Accordingly, these studies did not, however, determine the fraction of newly synthesized *lgp* that reached lysosomes via the plasma membrane. While recent pulse–chase experiments suggest that in MDCK cells the bulk of at least one *lgp*-like molecule appears at the basolateral plasma membrane before reaching lysosomes, quantitative interpretation is limited by the fact that “surface appearance” was determined after antibody addition at 37°C and could not be distinguished from antibody binding in endosomes (Nabi et al., 1991).

Transport via the cell surface to lysosomes has also been observed in stably transfected BHK cells overexpressing human lysosomal acid phosphatase (LAP), a soluble lysosomal enzyme that is transported as a membrane protein precursor (Braun et al., 1989). However, kinetic data seem to indicate that LAP, which is not a member of the *lgp120* family, is likely to reach lysosomes by a route distinct from *lgp*'s. Whereas molecules such as *lgp120* are transported to lysosomes with a $t_{1/2}$ of ~30 min, LAP reaches lysosomes with a $t_{1/2}$ of 5–6 h and is recycled repeatedly between the plasma membrane and endosomes en route.

A potential plasma membrane intermediate in *lgp* transport from the TGN to lysosomes is also indirectly implied by the fact that all *lgp*'s, like many plasma membrane receptors (Davis et al., 1986; Jing et al., 1990; Lobel et al., 1989), contain conserved cytoplasmic domain tyrosine residues that may serve as signals for rapid endocytosis (Kornfeld and Mellman, 1989; Ktistakis et al., 1990). Thus, *lgp-A* or LAP mutants in which this tyrosine was altered accumulate on the cell surface and cannot be internalized (Peters et al., 1990; Williams and Fukuda, 1990). While the failure of rapid endocytosis might account for the inability of these mutants to reach lysosomes, it is also possible that the conserved tyrosine residue plays a role in intracellular sorting, perhaps reflecting the accumulation of *lgp*'s in clathrin-coated buds in the TGN. Interestingly, all *lgp*'s also contain a conserved glycine residue on the amino-terminal side of the tyrosine; the significance of this residue for targeting to lysosomes is unknown.

We have generated a series of stably transfected CHO cell lines selected for different expression levels of wild-type *lgp120* or various cytoplasmic domain mutants. Using several independent assays to selectively monitor the kinetics of surface appearance vs. internalization of newly synthesized *lgp*'s, we have been able to better define the extent to which *lgp*'s pass through the plasma membrane en route to lysosomes and the factors that regulate cell surface transport. We have found that under normal conditions, most of the *lgp* is sorted intracellularly and reaches lysosomes without appearing on the plasma membrane. However, intracellular sorting can be rendered less efficient, and the degree of surface transport increased, by amplifying the level of *lgp* expression or by cytoplasmic domain mutations that more severely affect targeting from the TGN than endocytosis.

Materials and Methods

Cell Culture and Transfection

NRK fibroblasts were maintained in DME containing 5% FBS. CHO-K1

were grown in α -MEM supplemented with 10% FBS. CHO cell lines deficient in dihydrofolate reductase, DUKX-B11 and DG44, were obtained from Dr. L. Chasin (Columbia University, NY). The untransfected mutant cells were maintained in α -MEM supplemented with nucleosides and 10% FBS. All cells were grown at 37°C in 5% CO₂ in the presence of 100 U/ml penicillin and 100 μ g/ml streptomycin. CHO cells were stably transfected with 10 μ g plasmid DNA/10-cm tissue culture dish of 30% confluency by the calcium phosphate precipitation technique (Wigler et al., 1979). On day 2 after transfection, cells were dissociated with trypsin/EDTA and plated in selective medium containing 600 μ g/ml G418 (Gibco BRL, Gaithersburg, MD; CHO-K1) or in α -MEM without nucleosides supplemented with 10% dialyzed FBS (DUKX-B11 and DG44). To amplify expression, DUKX-B11 cells, transfected with pMT21 wild-type *lgp120* DNA, were plated in selection medium containing 4 μ g/ml folic acid and 0.1 μ M methotrexate (Lederle Parenterals, Inc., West Grove, PA). Stable cell lines were obtained by subcloning of single colonies or by limiting dilution 14 d after transfection. For most experiments, cells were plated out 24–48 h before use.

Oligonucleotide-directed Mutagenesis and Plasmid Construction

Mutations in the cytoplasmic tail of *lgp120* were generated by oligonucleotide-directed mutagenesis using the method of Kunkel (1985) as described in the Bio-Rad mutagenesis instruction manual (Bio-Rad Labs.-Chem. Div., Richmond, CA). Mutagenic 20-base oligonucleotides were used in which the codon for the cytoplasmic glycine residue located at position 7 was changed to an alanine residue or the codon for a tyrosine residue at position 8 was changed to a cysteine residue. The mutations were verified by dideoxynucleotide sequencing (Sanger et al., 1977) using the Sequenase kit (Un. States Biochem. Corp., Cleveland, OH) according to the manufacturer's instructions. EcoRI–HindIII fragments containing the cDNA coding for wild-type or mutant rat *lgp120* were excised from the vectors M13mpl9 or M13mpl8. EcoRI linkers were added to the fragments which were then cloned into a single EcoRI site of the plasmid vector pFRCMneo (pFRSV derivative, map available upon request; Horwich et al., 1985) located downstream from the SV40 origin of replication or into pMT21 downstream from an adenovirus major late promoter (Kaufman, 1990a).

Metabolic Labeling, Surface Biotinylation, and Immunoprecipitation

Cells grown in 35-mm dishes to a confluency of ~75% were metabolically labeled for 12–16 h with 0.5 mCi/ml of each ³⁵S-translabel (Trans³⁵S-label; ICN Biomedicals Inc., Costa Mesa, CA) and [³⁵S]cysteine (Amersham Corp., Arlington Heights, IL) in cysteine- and methionine-free MEM (MEM Select-Amine Kit, Gibco BRL) supplemented with 10% dialyzed FBS, 20 mM HEPES, pH 7.4, 1.5 μ g/ml methionine, and 2.4 μ g/ml cysteine. Monolayers were washed six times over a period of 20 min with ice-cold PBS⁺⁺ before adding sulfo-NHS-SS-biotin (Pierce Chemical Co., Rockford, IL) at a concentration of 1.5 mg/ml in PBS⁺⁺ for 30 min on ice. After washing six times with 50 mM glycine in PBS⁺⁺, the cells were lysed with 1% Triton X-100 in 100 mM sodium phosphate, pH 8.0, containing protease inhibitors (0.3 U/ml aprotinin, 1 mM PMSF, 10 μ g/ml pepstatin A, 10 μ g/ml leupeptin) for 30 min on ice. Postnuclear supernatants were obtained after two centrifugation steps of 10 min at 500 g and 30 min at 16,000 g and precleared with *Staphylococcus aureus* Wood 46 (Zymed Labs Inc., South San Francisco, CA). All immunoprecipitations were carried out in two steps. The first round was performed with a polyclonal rabbit anti-rat *lgp120* antiserum and protein A–Sepharose (Pharmacia LKB Biotechnology Inc., Piscataway, NJ). After washing and dissociation of antibody–antigen complexes by boiling in 0.5% SDS in PBS for 10 min and quenching with Triton X-100 to a final concentration of 0.4% SDS and 2% Triton X-100, a second round of precipitation was performed. To determine the amount of surface-biotinylated *lgp120* vs. total *lgp120*, one third of the eluted material was reprecipitated with the antibody and protein A–Sepharose; the other two thirds were precipitated with streptavidin–agarose (Sigma Chemical Co., St. Louis, MO). SDS-PAGE was carried out on 8% acrylamide gels under reducing conditions. Dried gels were exposed to x-ray film and protein bands were quantified by digitization using a Visage 2000 image processor (Eastman Kodak Co., Rochester, NY) supported by a Sun Microsystems workstation.

Cell Surface Transport Assays

CHO cells grown in 35-mm dishes to a confluency of 85–95% were starved

in MEM lacking cysteine and methionine (MEM Select-Amine Kit, Gibco BRL) for 30 min in a 37°C incubator. Cells were then pulse labeled with 3 mCi/ml ³⁵S-translabel (Tran³⁵S-label; ICN Biomedicals Inc., Costa Mesa, CA) and [³⁵S]cysteine (Amersham Corp.) for 15 min at 37°C. After washing twice with prewarmed complete medium containing a twofold excess of cysteine (0.3 mM) and methionine (0.3 mM), cells were chased for different periods of time. For surface biotinylation, the same protocol was used at each time point as described above. Cell surface immunoprecipitation was performed at each time point by incubating cells on ice for 2 h in a 1:50 dilution of anti-Igpl20 antiserum in complete medium. Cells were then washed six times with PBS⁺⁺ containing 1% BSA over a 30-min period, and twice with PBS without BSA followed by detergent lysis. After preclearing of the postnuclear supernatants with fixed, protein A-negative *S. aureus* Wood 46, the lysates were divided into two aliquots. Igp that appeared on the surface and thus bound antibody was precipitated from two thirds of the lysate by the addition of protein A-Sepharose. Total Igp was precipitated by supplementing one third of the lysate with additional anti-Igpl20 antiserum and protein A-Sepharose. After washing, the antibody-antigen complexes were dissociated by boiling in SDS and a second round of immunoprecipitation was performed as described above. Surface precipitation and biotinylation procedures recovered surface Igpl20 at equivalent efficiencies.

Endocytosis Assays

To monitor internalization by immunofluorescence, living cells grown on glass coverslips were incubated with hybridoma culture supernatant containing the mouse monoclonal anti-rat Igpl20 antibody Ly1C6 IgG (Lewis et al., 1985) for 2 h on ice or at 37°C. Cells incubated on ice were washed three times with PBS containing 10% goat serum to remove excess antibody before warming to 37°C for 30 min or 1 h to allow internalization. Cells were then fixed with paraformaldehyde-lysine-periodate (McLean and Nakane, 1974) for 1 h at room temperature after permeabilization with 0.01% saponin in PBS for 7 min and labeling with an affinity-purified, Texas red-conjugated goat anti-mouse IgG (Jackson ImmunoResearch Labs., Inc., West Grove, PA). After extensive washing with PBS containing 10% goat serum, cells were mounted in Mowiol and viewed with an Axiophot microscope (Carl Zeiss, Inc., Thornwood, NY). Pictures were taken with Tri-X Pan film (Eastman Kodak Co.) developed at 1,600 ASA. Quantitative and kinetic analysis of internalization were performed using ¹²⁵I-labeled Ly1C6 IgG. Cells grown in 35-mm dishes were incubated with ¹²⁵I-Ly1C6 at a concentration of 1 µg/ml in complete medium for different periods of time at 37°C or for 2 h on ice. To remove excess antibody, cells were washed six times with ice-cold PBS containing 1% BSA over a period of 30 min. Cells incubated with ¹²⁵I-Ly1C6 on ice were subsequently warmed to 37°C for various times. Cells were then cooled on ice and treated twice with 0.5 M acetic acid in 0.15 M NaCl, pH ~2.5, for 7 min. This procedure removed 75–85% of the ¹²⁵I-Ly1C6 bound at 4°C without subsequent warming. Internalized antibody was defined as the fraction of antibody initially bound that was resistant to removal by the low pH wash. Specific internalization was determined by subtracting the amount of ¹²⁵I-Ly1C6 bound in the presence of a 150-fold excess of unlabeled Ly1C6 IgG. Endocytosis of metabolically labeled cells was analyzed using the protocol for surface biotinylation with sulfo-NHS-SS-biotin as described above. After quenching excess biotin, cells were incubated at 37°C in complete medium for 30 min or 1 h. Cells were then cooled on ice and treated three times for 10 min with 50 mM glutathione in 0.075 M NaCl, 0.01 M EDTA containing 1% BSA and 0.075 N NaOH at 4°C (Bretscher and Lutter, 1988). Excess glutathione was quenched with 5 mg/ml iodoacetamide in PBS before cell lysis. Glutathione treatment removed 95–100% of the biotinylated Igpl20. Biotinylated Igp was precipitated as described above. Internalization was defined as the amount of Igpl20 immunoprecipitated after glutathione treatment compared to Igpl20 immunoprecipitated from a nontreated control. Quantitation of the glutathione-resistant Igpl20 was performed by digital densitometry.

Immunofluorescence Microscopy

Cells were plated out on glass coverslips 2 d before the experiment and grown to a confluency of 30%. To detect rat Igpl20, a polyclonal rabbit anti-rat Igpl20 antiserum or the mouse monoclonal anti-rat Igpl20 antibody Ly1C6 was used (Lewis et al., 1985). For labeling of hamster Igp95, the mouse monoclonal anti-hamster antibody E9A IgG was used (Schmid, S., R. Fuchs, and I. Mellman, unpublished procedure). An affinity-purified, polyclonal rabbit antipeptide antibody specific for the 11-amino acid cytoplasmic domain of wild-type Igp-A was used for double-labeling experiments. For surface labeling, living cells were incubated with the pri-

mary antibody diluted in medium containing 10% FBS and 20 mM Hepes, pH 7.4, or directly with the hybridoma culture supernatant. After washing off excess antibody with PBS containing 10% goat serum, cells were fixed with paraformaldehyde-lysine-periodate (McLean and Nakane, 1974) and incubated with an affinity-purified fluorescent secondary antibody. To localize intracellular antigen, cells were permeabilized with 0.01% saponin in PBS for 7 min at room temperature before adding the antibody. Coverslips were mounted in Mowiol and viewed with an Axiophot microscope. Pictures were taken with Tri-X Pan film and developed at 1,600 ASA.

Results

Since transient expression of cDNAs yields highly variable amounts of protein and can alter intracellular transport due to lytic effects of viral-based expression systems, we generated stable, Igpl20-expressing cell lines using nonviral plasmid vectors. CHO cell lines expressing different amounts of the transfected protein were obtained by using two different expression vectors with or without drug-induced amplification. pFRCMneo, a cytomegalovirus-based derivative of pFRSV (Miettinen et al., 1989) containing the neomycin resistance gene, yielded expression levels of the transfected Igp similar to or lower than the amount of Igpl20 produced endogenously by NRK cells. The second vector, pMT21, utilizes the adenovirus major late promoter (Kaufman, 1990a). Since both vectors contained a wild-type dihydrofolate reductase gene as a selectable marker, expression could be enhanced by growing the cells in the presence of increasing concentrations of methotrexate (Kaufman, 1990b; Miettinen et al., 1989). pMT21-transfected clones were chosen that expressed the transfected wild-type Igpl20 over a 1 to >15-fold range compared to NRK Igpl20. Expression was quantified by metabolic labeling, followed by quantitative immunoprecipitation, SDS gel electrophoresis, and computer-assisted digitization of the autoradiograms.

Wild-Type Igpl20 Can Be Detected on the Cell Surface Only in High Expressing, Transfected Cells

The distribution of transfected rat wild-type Igpl20 in CHO cells was first monitored by immunofluorescence microscopy and compared with endogenous rat Igpl20 in NRK cells. For cell surface staining, live cells were incubated with a rat-specific anti-Igpl20 antiserum on ice followed by fixation and labeling with a fluorescent secondary antibody. Intracellular Igpl20 was visualized after fixation and permeabilization of the cells. As shown, NRK cells (Fig. 1, A and B), and transfected CHO cells expressing low levels of Igpl20 (Fig. 1, C and D), did not have detectable amounts of the protein on the cell surface. However, in transfected CHO cells expressing higher amounts of the protein, cell surface staining was clearly visible (Fig. 1, E and F).

To quantify the fraction of total rat Igp on the plasma membrane at steady state, surface Igp molecules were selectively derivatized by the membrane-impermeant probe sulfo-NHS-SS-biotin. Cells were labeled to equilibrium with [³⁵S]cysteine and [³⁵S]methionine followed by surface biotinylation on ice. After cell lysis, total Igp was precipitated with a polyclonal antibody specific for rat Igpl20 and the resulting immunoprecipitates were divided into two aliquots. Biotinylated "surface Igp" was precipitated from one aliquot corresponding to two thirds of the lysate using immobilized streptavidin; "total Igp" was precipitated from one third by a second round of immunoprecipitation. Total and

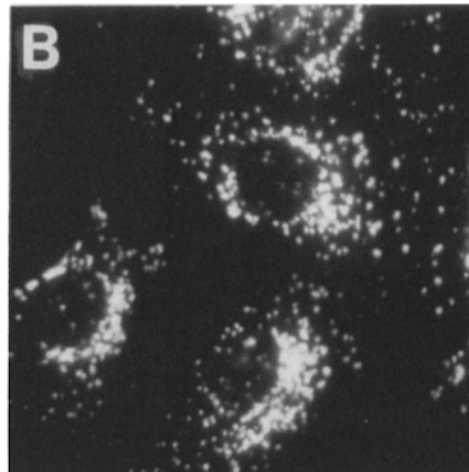
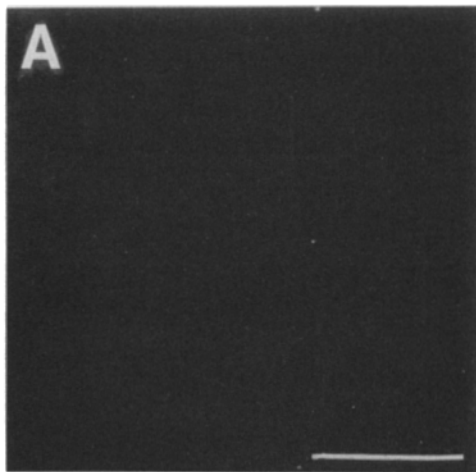
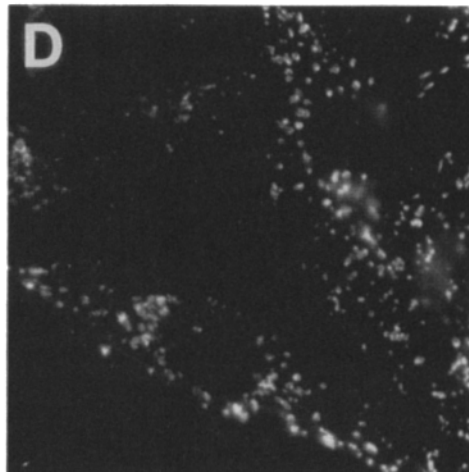
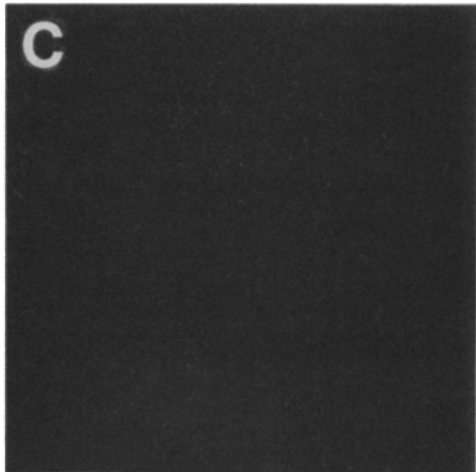
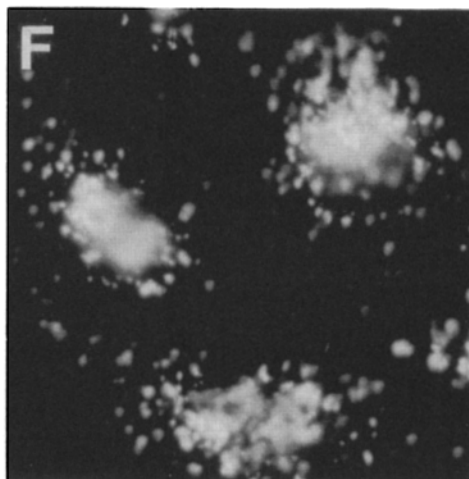
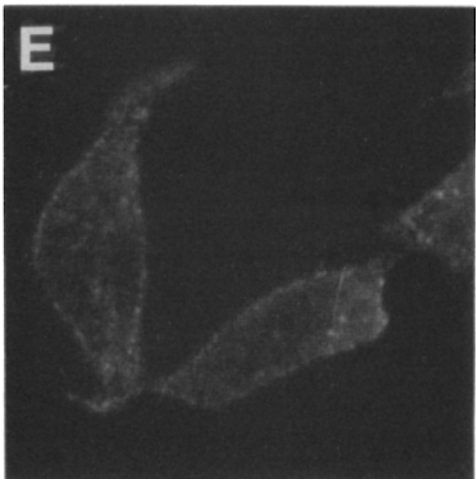
SURFACE**PERMEABILIZED****endogenous
wtlgp120
NRK cells****transfected
wtlgp120
low expression****transfected
wtlgp120
high expression**

Figure 1. Immunofluorescence localization of rat wild-type lgp120 in NRK and transfected CHO cells. For surface labeling, living cells were incubated with a rabbit anti-rat lgp120 antiserum for 2 h on ice before fixation. For staining of total (surface + intracellular) rat lgp120, cells were fixed and permeabilized before labeling with a rabbit anti-rat lgp120 antiserum. Affinity-purified, Texas red-conjugated IgG was used as a secondary antibody. (A) Surface labeling of endogenous lgp120 in NRK cells. (B) Total lgp120 in permeabilized NRK cells. (C) Surface labeling of transfected, low expressing CHO cells. (D) Total rat lgp120 in transfected, low expressing CHO cells. (E) Surface labeling of transfected, high expressing CHO cells. (F) Total rat lgp120 in transfected, high expressing CHO cells. Relative levels of lgp120 expression are given in Fig. 2. Bar, 5 μ m.

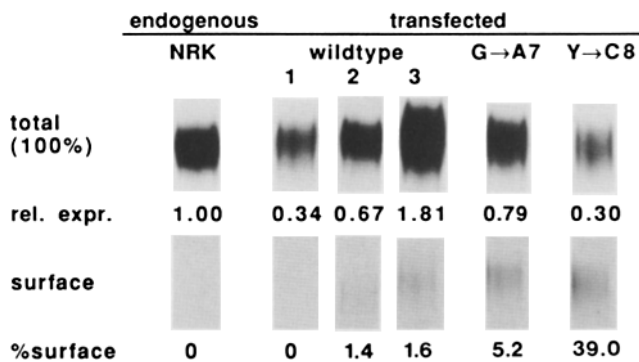


Figure 2. Cell surface distribution of wild-type and mutant lgp120. Equal numbers of cells were labeled with [³⁵S]methionine and [³⁵S]cysteine overnight, washed, and subjected to surface biotinylation using sulfo-NHS-SS-biotin for 30 min on ice. Biotinylated cells were lysed in Triton X-100, and total lgp120 was immunoprecipitated with anti-rat lgp120 antiserum, and the immune complexes were dissociated from the immunoabsorbent by boiling in SDS. Samples were divided in aliquots of one third for reprecipitation of total lgp120 with anti-lgp120 antiserum and immobilized protein A (*total*), and two thirds for precipitation of biotinylated lgps with streptavidin-agarose (*surface*). Quantification was done by computer-assisted digitization of autoradiograms using a Visage 2000 image processor (Eastman Kodak Co.). Total ³⁵S-labeled lgp120 is expressed relative to the amount of endogenous NRK lgp120 (defined as a relative expression level = 1). Surface biotinylated ³⁵S-labeled lgp120 was expressed as the percentage of total ³⁵S-labeled lgp120, after correcting for differences in aliquot size.

biotinylated lgp were quantified after SDS-PAGE and digital analysis of resulting autoradiograms. To provide a basis for comparison, total amounts of rat lgp120 in the transfected cell lines were expressed relative to endogenous NRK lgp120. These results are shown in Fig. 2.

In agreement with the fluorescence microscopy, no biotinylated rat lgp120 was detectable on the surface NRK cells or CHO cells expressing low levels (clone 1, relative expression = 0.34). However, in cell lines expressing higher amounts of the transfected lgp (clones 2 and 3), the biotinylated rat lgp120 accounted for 1.5% of the total immunoprecipitable ³⁵S-labeled lgp120.

Endogenous lgp-B Also Reaches the Cell Surface in CHO Cells Overexpressing Rat lgp120

The increased amounts of surface lgp120 on cells expressing higher levels of the transfected protein might reflect an enhanced ability to detect a small but constant fraction of protein on the plasma membrane. However, since surface lgp120 was not observed in NRK cells which expressed more of the protein than some of the CHO transfectants (e.g., Fig. 2, clone 2), sensitivity of the biotinylation assay was not a limiting factor. Alternatively, surface expression might have resulted from the saturation of a intracellular sorting site needed for delivery of lgp120 from the TGN to endosomes or lysosomes. If true, such a situation might also be expected to result in the partial missorting of endogenous lgp's in CHO cells which presumably compete for the same, limited capacity sorting apparatus. To test this possibility, we examined the distribution of lgp95 (lgp-B) in cells expressing different amounts of the transfected protein.

In nontransfected cells, lgp95 is normally undetectable on

the cell surface by immunofluorescence or biochemical labeling (not shown). Similarly, in cells expressing low levels of transfected lgp120, neither the transfected lgp120 (Fig. 3 A) nor lgp95 was detected on the plasma membrane (Fig. 3 B); both transfected and endogenous lgp's colocalized intracellularly (Fig. 3, C and D). However, in cells expressing levels of rat lgp120 that lead to the appearance of the transfected protein on the cell surface, plasma membrane lgp95 was also detected (Fig. 3, E and F). Labeling of lgp95 on the cell surface was not the result of cross reaction with secondary antibodies, since similar results were obtained using single labeling. Moreover, the anti-lgp95 antibody was found not to react with the transfected rat lgp120, since it failed to detect rat lgp120 in permeabilized NRK cells (not shown) and did not detect the precise pattern observed using rabbit anti-lgp120 in transfected cells (Fig. 3, G and H). In summary, these results suggest that upon overexpression of lgp120 in transfected cell lines, both the transfected and endogenous lgp may be missorted to the cell surface.

Differential Effect of Cytoplasmic Tail Mutations on Lysosomal Transport

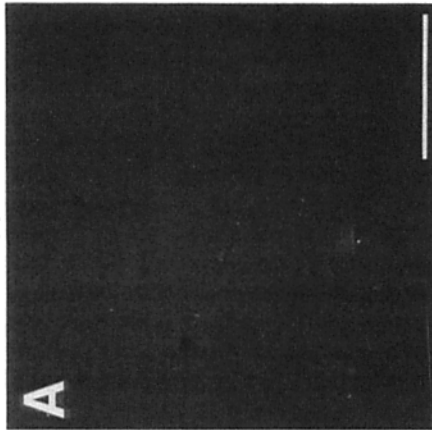
Whether lgp's are delivered to lysosomes directly from the TGN or after internalization from the cell surface, it is clear that they must contain one or more sorting determinants that specify their intracellular transport. At least one important determinant is in the lgp cytoplasmic domain, since replacement of the cytoplasmic tail tyrosine residue at position 8 (Y8) of human lamp-1 (lgp-A) has been shown to result in its transport to the cell surface in transfected COS cells (Williams and Fukuda, 1990). However, although this tyrosine is needed for endocytosis, it is unclear whether it also has a role in targeting from the Golgi complex. Another factor that may play a role in lgp transport is the glycine residue at position 7 (G7) that is also conserved in all known lgp's.

We investigated the role of the glycine-tyrosine motif in lysosomal targeting by generating stable CHO cell lines expressing the cytoplasmic tail mutants lgp120Y→C8 and lgp120→A7 at relatively low levels to exclude missorting due to overexpression. Nevertheless, in both cell types, the mutant lgp's were found at the plasma membrane after antibody labeling of live cells at 4°C by immunofluorescence (Fig. 4, A and C). While little of the tyrosine mutant was found in intracellular vesicles (Fig. 4 B), a significant fraction of the glycine mutant gave a typical lysosome-like staining pattern (Fig. 4 D). We next quantified the extent of plasma membrane expression of both mutants and found that lgp120Y→C8 was almost eightfold more accessible to surface biotinylation than lgp120G→A7, 39% vs. 5.2% of the amount of immunoprecipitated lgp120, respectively (Fig. 2). Both of these values were considerably higher than obtained for even high expressing wild-type lgp120 transfectants (1.5%).

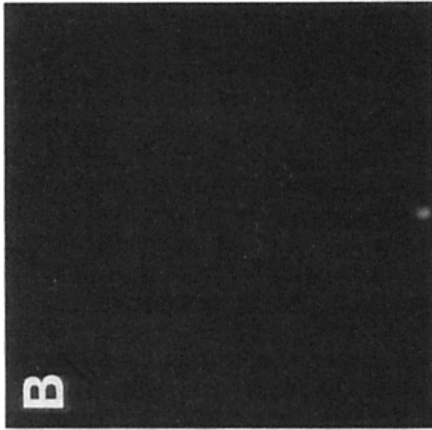
To determine whether the intracellular lgp120G→A7 colocalized with endogenous lgp-A, permeabilized cells were stained using the rat-specific mouse monoclonal antibody Ly1C6 IgG and an affinity-purified rabbit antitail peptide lgp-A antibody. While the antipeptide antibody detected endogenous lgp-A in CHO cells, it did not react with either cytoplasmic domain mutant. As shown in Fig. 5, the intracellular staining due to lgp120G→A7 (anti-rat lgp120) exhibited significant colocalization with staining due to endogenous CHO cell lgp-A (antitail lgp-A). A fraction of lgp120G→A7

SURFACE

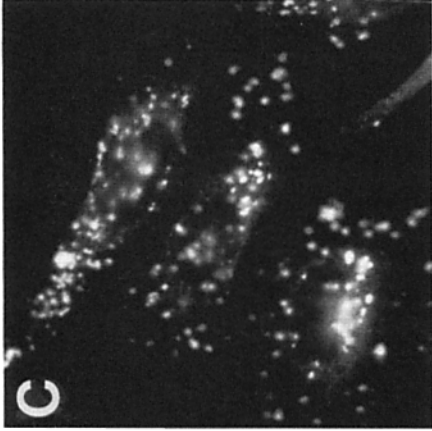
Igp120



Igp95



Igp120



Igp95

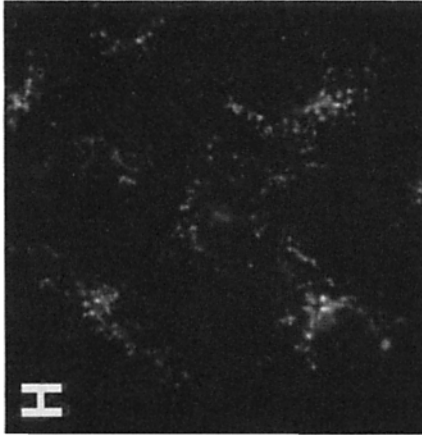
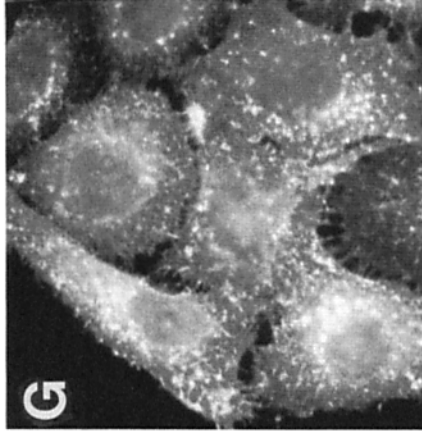
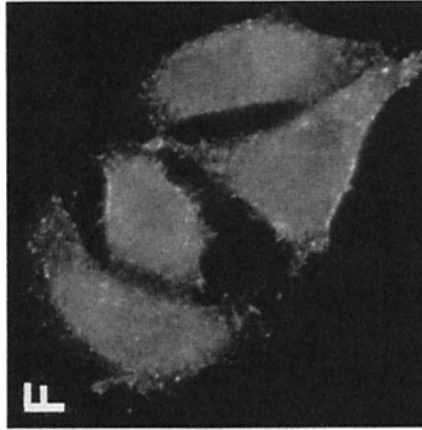
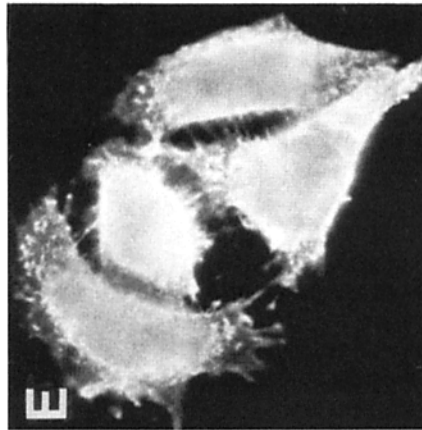
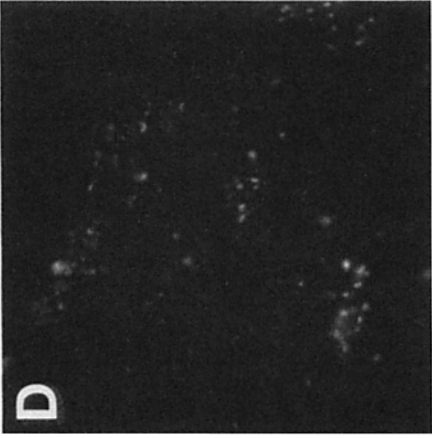


Figure 3. Distribution of endogenous hamster Igp95 (Igp-B) and transfected rat Igp120 in CHO cells. CHO cells producing either low (A-D) or high (E-H) levels of rat Igp120 were analyzed for the surface vs. intracellular distributions of the transfected rat Igp120 (Igp-A) and endogenous hamster Igp95 (Igp-B). To detect Igp's present on the plasma membrane, live cells were double labeled at 0°C with a rat-specific rabbit anti-Igp120 antiserum (A and E) and a hamster-specific mouse monoclonal anti-Igp95 antibody (E9a IgG) (B and F). Surface Igp120 and Igp95 was only detected on CHO cells overexpressing the transfected rat Igp120 (E and F). For labeling of total Igp's, cells were fixed and permeabilized before incubation with the anti-rat (C and G) or hamster (D and H) antibodies. Affinity-purified fluorescein-conjugated goat anti-mouse and Texas red-conjugated goat anti-rabbit IgGs were used as secondary antibodies. In control experiments in which the anti-Igp120 vs. anti-Igp95 were used alone and/or in combination with the incorrect second antibody, we established that neither the first nor second antibodies exhibited cross-reactivity under the conditions used here. Bar, 5 μ m.

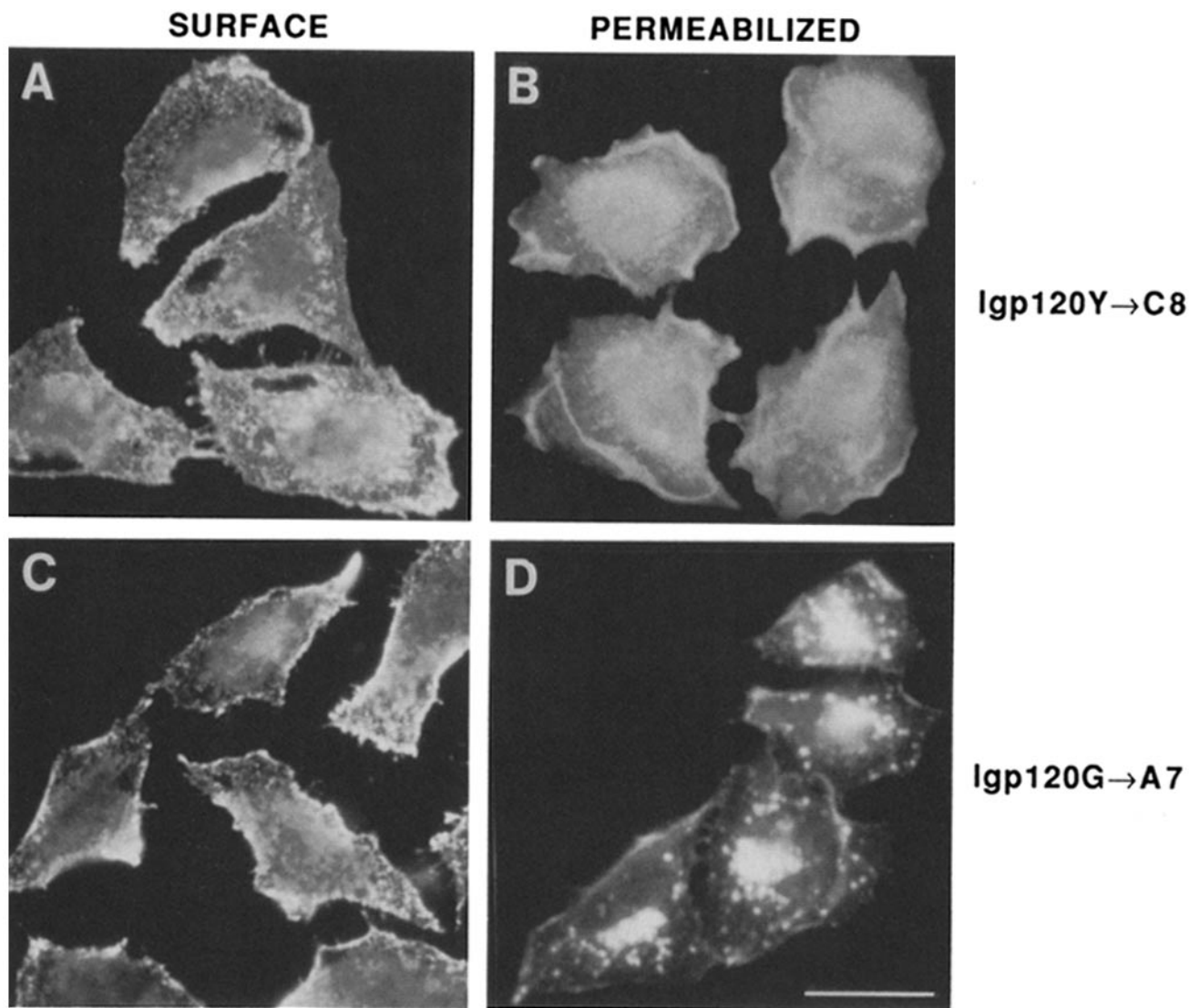


Figure 4. Immunofluorescence localization of Igpl20Y→C8 and Igpl20G→A7 in transfected CHO cells. Cells expressing either the Igpl20Y→C8 (A and B) or Igpl20G→A7 (C and D) mutants were stained for cell surface (A and C) or intracellular (B and D) rat Igpl20 using a rabbit anti-rat Igpl20 antiserum as described in the legend to Fig. 1. Bar, 5 μ m.

mutant was also detected at the cell surface that was not detected by the antitail peptide antibody. Virtually all of the Igpl20Y→C8 mutant exhibited a diffuse surface staining pattern that was entirely distinct from the pattern of endogenous Igpl-A distribution. The fact that the two patterns were so different emphasizes the distinct specificities of the two antibodies.

These observations thus indicate that the conserved glycine and tyrosine residues of the rat Igpl20 cytoplasmic domain contributed differentially to lysosomal targeting. While removing the tyrosine residue abolished lysosomal transport and resulted in cell surface localization, substitution of the glycine residue only partially interfered with lysosomal targeting.

Endocytosis of Igpl20 Requires Only the Cytoplasmic Tail Tyrosine Residue

If the normal pathway of Igpl20 transport to lysosomes required transit through the plasma membrane, then the dual

localization of Igpl20G→A7 on the cell surface and in lysosomes might be explained by a much slower rate of internalization due to the mutation of the cytoplasmic tail glycine. To test this possibility, we next compared the kinetics of endocytosis of Igpl20G→A7 and wild-type Igpl20.

Internalization was first monitored by immunofluorescence. Cells were incubated for 2 h at 37°C in medium containing the anti-Igpl20 mAb Ly1C6 IgG. As shown in Fig. 6, antibody bound to cells overexpressing wild-type Igpl20 (Fig. 6 A) or expressing Igpl20G→A7 (Fig. 6 B) was internalized and delivered to intracellular vesicles typical of late endosomes and lysosomes. Uptake was similar for both cell lines, although a small amount of surface staining remained in the case of the cells expressing the glycine mutant. In contrast, cells expressing the Igpl20Y→C8 mutant were incapable of delivering anti-Igpl20 antibody to intracellular vesicles, with all cell-associated Ly1C6 remaining at the plasma membrane (Fig. 6 C). Importantly, even after prolonged incubations at 37°C, neither binding nor internalization was observed in CHO cells expressing low levels of wild-type

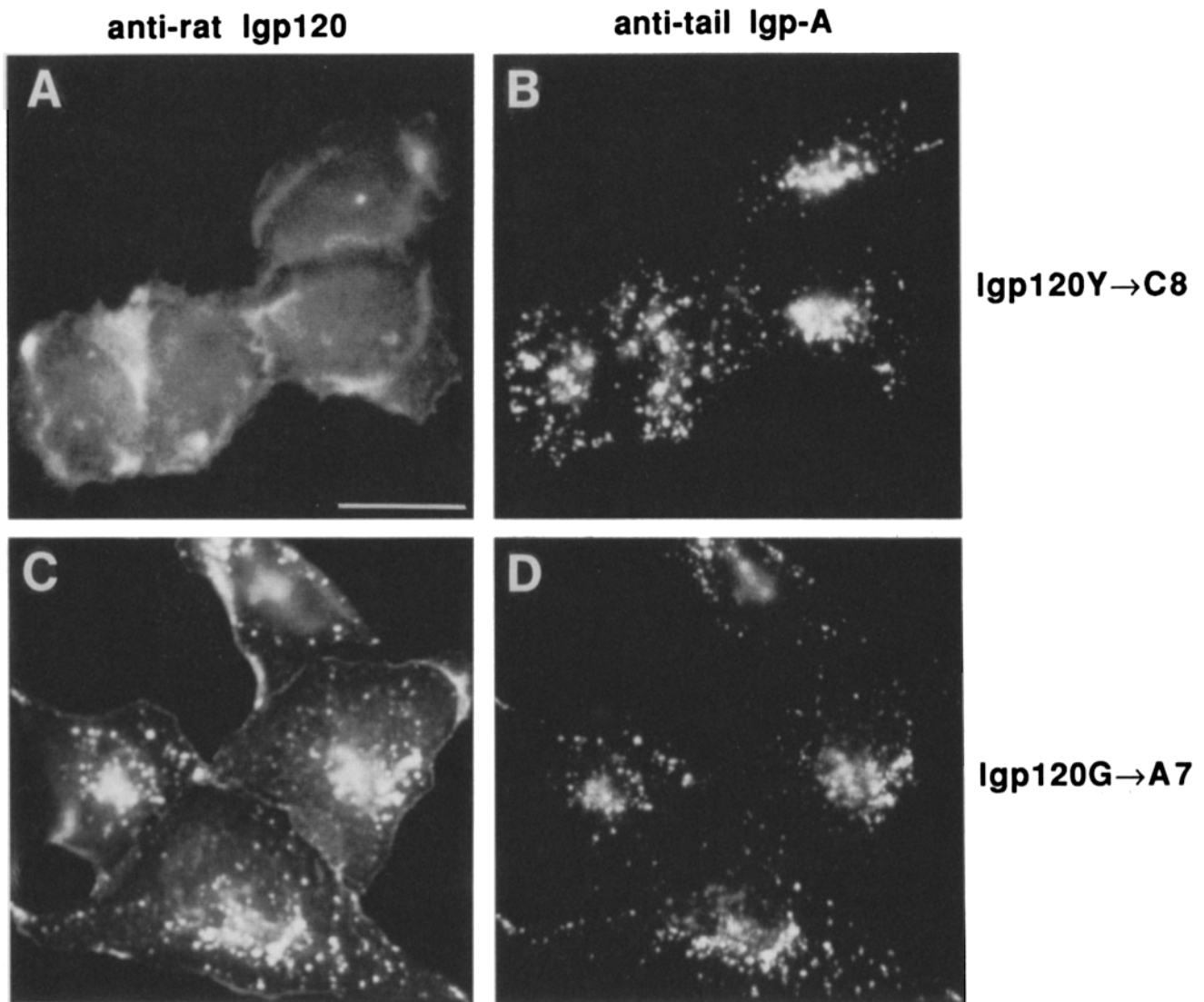


Figure 5. Colocalization of Igp120Y→A8 or Igp120G→A7 with endogenous Igp-A. Permeabilized CHO cells expressing Igp120Y→A8 (A and B) and Igp120G→A7 (C and D) mutants were double labeled with the rat-specific mouse monoclonal anti-Igp120 antibody Ly1C6 IgG (A and C) or with a rabbit antitail Igp-A peptide antiserum (B and D) followed by staining with the appropriate fluorescein-conjugated anti-rabbit and Texas red-conjugated anti-mouse secondary antibodies. Although peripheral surface staining was observed for both mutant transfectants using Ly1C6 IgG, this pattern was not visualized using the antitail peptide antibody which was thus judged to react only with endogenous wild-type CHO Igp-A in endosomes and lysosomes. Bar, 5 μ m.

Igp120 (clone 1) (Fig. 6 D); similar results were obtained for nontransfected CHO cells (not shown) and NRK cells (not shown). Thus, Igp120G→A7 bound and internalized externally added antibody in a manner qualitatively similar to overexpressed wild-type Igp120, suggesting that the increased expression of Igp120G→A7 at the cell surface did not reflect an endocytosis defect. Moreover, the failure of NRK cells and low expressing wild-type transfectants to internalize antibody suggested that Igp120 reached lysosomes in these cells without becoming accessible to externally added antibody.

To confirm the immunofluorescence results quantitatively and to obtain actual rates of endocytosis, we next determined the kinetics of internalization. Cell monolayers were incubated in 125 I-Ly1C6 IgG at 37°C for various lengths of time in the presence or absence of excess unlabeled antibody

and internalized (acid-resistant) antibody determined. As shown in Fig. 7, cells expressing the wild-type protein or Igp120G→A7 internalized equivalent percentages of 125 I-Ly1C6 IgG after 30 min, although the initial rate of uptake for the wild-type protein was somewhat faster than for the glycine mutant. Both cell lines internalized 125 I-Ly1C6 IgG far more rapidly than did cells expressing the Igp120Y→C8 mutant (Fig. 7).

While the rate of internalization of 125 I-Ly1C6 IgG was comparable for both the overexpressed wild-type Igp120 and the Igp120G→A7 mutant, when normalized to the different levels of Igp120 expression in each cell line (Fig. 2), the absolute amount of antibody bound and taken up by cells expressing Igp120G→A7 was significantly higher. From the actual amounts of antibody measured in Fig. 7, cells expressing Igp120G→A7 bound and internalized 4.4×10^3 and $45.0 \times$

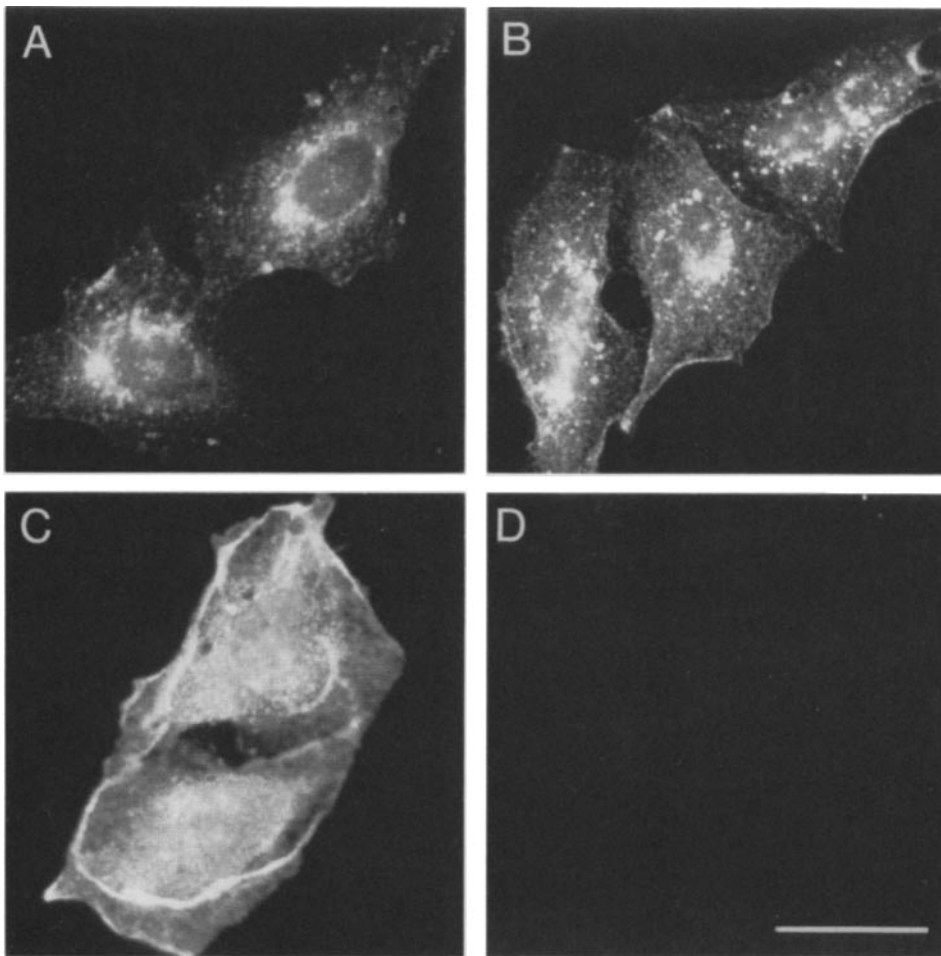


Figure 6. Immunofluorescence of internalized anti-rat Igpl20 antibody by CHO cells transfected with wild-type and mutant Igpl20. Transfected cells expressing wild-type Igpl20, Igpl20G→A7, and Igpl20Y→C8 were incubated in medium containing the anti-rat Igpl20 antibody LylC6 IgG (15 μ g/ml) for 2 h at 37°C. The cells were then washed on ice, fixed, permeabilized, and stained with a Texas red-conjugated anti-mouse antibody. (A) Wild-type CHO transfectants at high expression level. (B) Igpl20G→A7 CHO transfectants. (C) Igpl20Y→C8 CHO transfectants. (D) Wild-type CHO transfectants at low expression level.

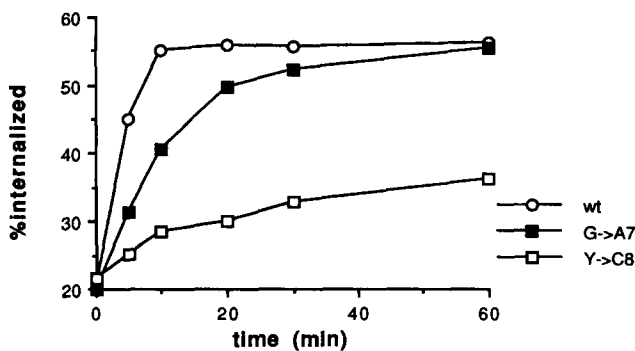


Figure 7. Kinetics of internalization of 125 I-LylC6 IgG by cells expressing wild-type or mutant Igpl20. Transfected cell lines were incubated with 125 I-LylC6 IgG (1 μ g/ml) for 2 h at 37°C in the presence or absence of 150-fold excess unlabeled antibody. The monolayers were then cooled on ice and washed to remove unbound antibody. Surface-bound antibody (acid-sensitive) was eluted by washing at low pH, followed by cell lysis to determine internalized (acid-resistant) radioactivity. Specific internalization was determined after subtracting 125 I-IgG bound and/or internalized in the presence of unlabeled LylC6. All data points represent the average of duplicate measurements of two independent experiments ($\pm 10\%$ variation).

10^3 cpm of 125 I-LylC6 IgG (respectively) as compared with 0.9×10^3 cpm bound and 15.9×10^3 cpm internalized for the wild-type transfectants. Thus, cells expressing the Igpl20G→A7 mutant were more efficient at binding and endocytosis of 125 I-LylC6 IgG, suggesting that a greater fraction of the mutant reached the cell surface than did the wild type.

Finally, to ensure that wild-type and glycine mutant Igpl20 were internalized comparably even in the absence of bound antibody, we measured Igpl20 endocytosis after surface biotinylation with sulfo-NHS-SS-biotin. After derivatization on ice, cell monolayers were warmed to 37°C for 30 or 60 min. Cells were then cooled and treated with glutathione to remove any biotin groups remaining on the cell surface. After cell lysis, total vs. biotinylated Igpl20 was determined. As illustrated in Fig. 8, comparable amounts of biotinylated Igpl20 were internalized in cells expressing the wild-type Igpl20 or Igpl20G→A7 mutant; relatively little protein was protected from reduction in cells expressing the Igpl20Y→C8 mutant. Quantitation yielded results similar to those obtained by antibody internalization: 23.4% of Igpl20G→A7 and 34% of wild-type Igpl20 were found intracellularly while the value for the Igpl20Y→C8 mutant was at the limit of detection of the assay (5.4%).

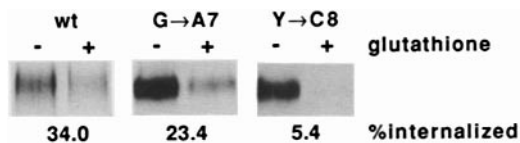


Figure 8. Internalization of surface biotinylated wild-type and mutant Igpl20. Transfected cell lines were metabolically labeled with [³⁵S]methionine and [³⁵S]cysteine overnight and subjected to cell surface biotinylation with sulfo-NHS-SS-biotin at 4°C. After quenching excess biotin reagent, cells were warmed to 37°C for 30 min to allow internalization. Cell surface-bound biotin was then removed by treatment of the cells with reduced glutathione. ³⁵S-labeled, biotinylated Igpl20 was precipitated with anti-rat Igpl20 antibody and protein A-Sepharose, followed by reprecipitation with streptavidin-agarose; precipitates were then analyzed by SDS-PAGE and autoradiography. Quantitation was performed using computer-assisted digitization of autoradiograms. The fraction of glutathione-resistant (% internalized) Igpl is expressed as percentage of precipitated Igpl from a control dish not subjected to glutathione treatment.

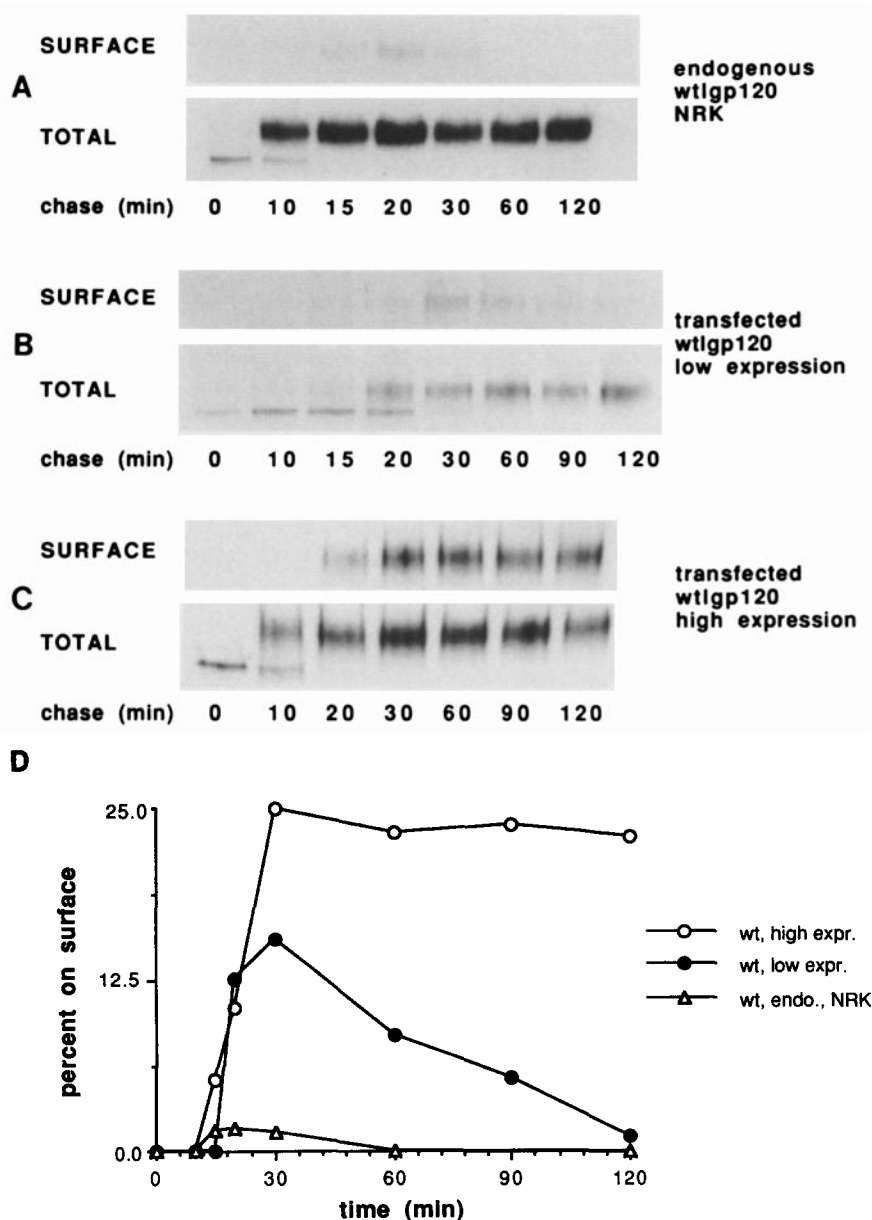


Figure 9. Surface appearance of newly synthesized wild type rat Igpl20 in NRK cells and transfected CHO cells. Cells were pulse labeled with [³⁵S]methionine and [³⁵S]cysteine for 15 min and then chased for the indicated times at 37°C. At each time point, the cells were placed on ice and labeled Igpl20 that had appeared on the surface derivatized using sulfo-NHS-SS-biotin or by the addition of a rabbit anti-rat Igpl20 antiserum at 4°C. Surface-biotinylated and total cell Igpl20 were precipitated from detergent lysates as described in the legend to Fig. 2. Antibody-labeled surface Igpl was precipitated after washing the cells to remove unbound antibody, by lysing the monolayers in Triton X-100 and then adding protein A-Sepharose to four fifths of the cell lysate; total Igpl was immunoprecipitated from one fifth by adding additional anti-Igpl20 antiserum. All precipitates were analyzed by SDS-PAGE and autoradiography; identical results were obtained using either the biotinylation or surface-bound antibody procedures. (A) Cell surface appearance of endogenous wild-type rat Igpl20 in NRK cells. (B) Transfected CHO cells expressing low levels. (C) Transfected CHO cells expressing rat Igpl20 at high levels. (D) Percentage of Igpl's detected on the cell surface relative to the total amount of immunoprecipitated Igpl's during the chase period as determined by computer-assisted digitization of autoradiograms and after correcting for differences in sample size. The results from two or three independent experiments were used for quantitation.

Together, these results show that Igpl20G→A7 is internalized somewhat more slowly than, but at an efficiency comparable with, wild-type Igpl20 in the presence or absence of antibody. Such a slight difference in endocytosis does not seem to be sufficient to account for the significant increase in the amount of surface Igpl20G→A7. Rather, the difference in surface expression implied that a greater fraction of newly synthesized Igpl20G→A7 than wild-type Igpl20 reached the plasma membrane after leaving the Golgi complex.

Newly Synthesized Wild-Type and Mutant Igpl's Reach the Plasma Membrane with Different Efficiencies

To determine directly the fraction of newly synthesized wild-type and mutant Igpl's arriving at the plasma membrane, we performed pulse-chase labeling combined with surface biotinylation or immunoprecipitation. Cells were pulse labeled for 15 min with [³⁵S]cysteine and [³⁵S]methionine and then chased for different periods of time. At each time point,

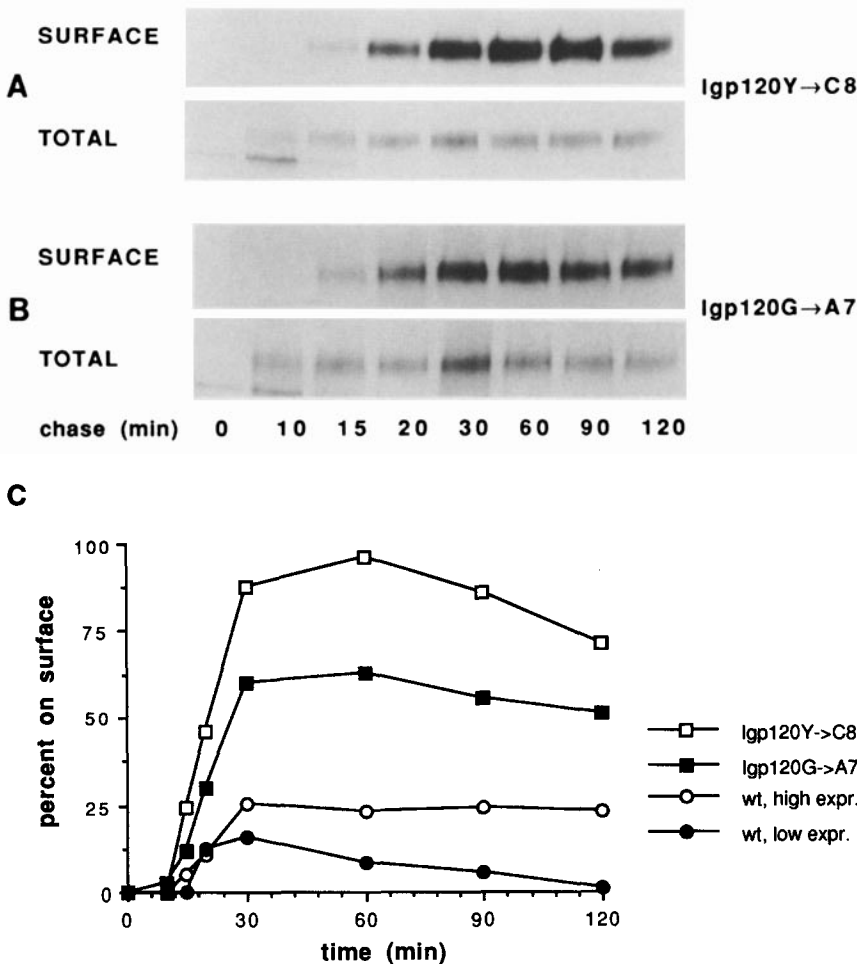


Figure 10. Surface appearance of Igpl20Y→C8 and Igpl20G→A7 in transfected CHO cells. Cells were treated as described in the legend to Fig. 9. Cell surface appearance of cells expressing Igpl20Y→C8 (A) or Igpl20G→A7 (B) was determined using cell surface biotinylation or antibody addition (not shown). (C) Percentage of Igpl's detected on the cell surface relative to the total amount of immunoprecipitated Igpl's during the chase period as determined by computer-assisted digitization of autoradiograms. Values for percent on surface were obtained after correcting for differences in sample size. The results from four (Igpl20Y→C8) or three (Igpl20G→A7) independent experiments were used for the quantitative analysis. Since 95% of newly synthesized Igpl20Y→C8 was found as having reached the plasma membrane, this mutant is likely to be transported almost quantitatively to the cell surface. Accordingly, we estimated that the biotinylation procedure was at least 95% efficient at recovering cell surface Igpl20.

surface appearance was detected by biotinylation of the cells at 0°C. As a control for the biotinylation procedure, each cell line was also examined by surface immunoprecipitation, in which cells were incubated on ice with a rat-specific rabbit anti-Igpl20 antibody followed by cell lysis and precipitation with protein A-Sepharose. Identical results were obtained from both procedures. After biotinylation or surface precipitation from four fifths of the initial lysate, total Igpl20 was determined by quantitative immunoprecipitation from an aliquot corresponding to one fifth of the cell lysate. The ratio of surface to total rat Igpl20 was determined by digitization of autoradiograms obtained after SDS-PAGE of the precipitates and surface Igpl expressed as a percentage of total after correcting for the differences in sample size.

In contrast to the results obtained after steady-state labeling (Fig. 2), pulse-chase labeling of NRK cells and transfected low expressing CHO cells demonstrated that a small, but reproducible fraction of newly synthesized wild-type Igpl20 was transported to the plasma membrane. Surface appearance in NRK cells was transient, reaching a maximum of 1.8% on the surface after 20 min, disappearing by 60 min (Fig. 9, A and D). A small but significantly greater fraction was detected transiently at the cell surface in CHO cells expressing low levels of rat Igpl20 (Fig. 9 B), reaching a maximum of 15% after 30 min of chase (Fig. 9 D). In cells expressing higher levels of Igpl20, an even greater fraction of newly synthesized protein was transported to the cell surface

reaching a maximum of 25% (Fig. 9, C and D). The kinetics of appearance were similar to the low expressing cells, but the fraction at the cell surface remained constant for 2 h, possibly reflecting the recycling of Igpl20 in overexpressing cells. In any event, these results suggested that a relatively small fraction of the total amount of newly synthesized Igpl20 reached the cell surface in cells expressing the wild-type protein. In transfected CHO cells, this fraction appeared to correlate with the total amount of Igpl20 made.

A different situation was observed for cells expressing either of the two mutant Igpl's. As shown in Fig. 10 A, Igpl20Y→C8 was rapidly and efficiently transported to the cell surface, becoming almost completely (95%) accessible to cell surface biotinylation or externally added antibody after 30 min (Fig. 10 C). Although not quite as efficient, most of the newly synthesized Igpl20G→A7 also reached the plasma membrane (Fig. 10 B), reaching a maximum of 65% (Fig. 10 C). This represented a much greater fraction of Igpl20G→A7 reaching the cell surface than was observed in the same cells expressing wild-type Igpl20 at levels comparable to or greater than the level of Igpl20G→A7 expression (Fig. 10 C). Moreover, since 95% of newly synthesized Igpl20Y→C8 was detected as having reached the plasma membrane, we conclude that the biotinylation procedure must be almost completely efficient at recovering all Igpl20 forms from the cell surface.

The kinetics of surface appearance of the mutant proteins

was similar to the wild-type protein, lgp first being detected by biotinylation or antibody addition after a lag of 10–15 min and reaching a maximum after ~30 min. As was the case for the overexpressed wild-type protein, a considerable fraction of the mutant lgp's reaching the cell surface was not cleared from the plasma membrane. In the case of the lgp120Y→C8 mutant, this probably reflected the relatively low rate of endocytosis. Since the overexpressed wild-type lgp120 and lgp120G→A7 were subject to rapid internalization (Figs. 6–8), their slow disappearance from the plasma membrane possibly reflected continuous recycling between the cell surface and one or more intracellular compartments.

Discussion

The issue of whether, or to what extent, lysosomal membrane glycoproteins such as lgp120 are transported from the TGN to lysosomes via an intracellular route or following endocytosis after insertion into the plasma membrane represents a critical unknown in our understanding of lysosomal biogenesis and Golgi apparatus function. Since the bulk of newly synthesized lysosomal enzymes bound to MPR appear to reach lysosomes without reaching the cell surface, it would appear likely that lysosomal membrane components take the same intracellular route (Kornfeld and Mellman, 1989). If lgp's indeed are targeted intracellularly, then they must contain one or more sorting determinants that prevent their transport to the cell surface and/or mediate their inclusion onto a specific pathway to lysosomes. Since lgp's do not contain mannose 6-phosphate residues (Howe et al., 1988), and since they bear no obvious sequence homology with MPR, it would be of clear importance to identify the nature of such sorting determinants.

In this paper, we have characterized several essential features controlling the transport of lgp120 which may help clarify some of the superficially conflicting data concerning the pathways of lgp to lysosomes. We have used a series of biochemical assays to specifically and quantitatively determine the fraction of lgp120 that appears on the cell surface. Our results show that only a very small fraction of the wild-type protein ever becomes accessible to labeling or antibody binding at the plasma membrane. This was true for rat lgp120 expressed endogenously in NRK cells or after transfection into CHO cells. However, surface appearance could be increased in one of two ways: first, by elevating the amount of lgp120 expression; and second by altering the lgp120 cytoplasmic domain.

Most importantly, mutation of either the conserved glycine or tyrosine residues resulted in the expression of proteins the majority of which appeared on the plasma membrane after exit from the Golgi complex. These results demonstrate that the assays used were capable of distinguishing efficient vs. inefficient transport of lgp120 to the plasma membrane. They also suggest that the lgp120 cytoplasmic domain contains a determinant that is important for directing transport to lysosomes via an intracellular route. Since the lgp120G→A7 mutant was capable of endocytosis from the plasma membrane, such a determinant is not identical to that required for rapid internalization nor is the increased surface appearance of lgp120G→A7 likely to be secondary to an internalization defect.

Table I. Summary of Cell Surface Expression, Rate of Plasma Membrane Insertion, and Endocytosis for Wild-Type and Mutant lgp120

Cell line	lgp on cell surface at equilibrium*	Newly synthesized lgp reaching surface†	Surface lgp internalized after 30 min‡
	%	%	%
NRK	0	1.8	0
CHO-wt, low	0	15.0	0
CHO-wt, high	1.5	25.0	35
CHO-G→A7	5.2	65.0	32
CHO-Y→C8	39.0	95.0	12

* Determined by overnight labeling with [³⁵S]methionine/cysteine followed by surface biotinylation; data taken from Fig. 2.

† Determined by pulse-labeling with [³⁵S]methionine/cysteine followed by surface biotinylation and surface precipitation at various times of chase; data taken from Figs. 9 and 10.

‡ Determined from the amount of ¹²⁵I-Ly1C6 IgG internalized after 30 min at 37°C; data taken from Fig. 7.

Intracellular Transport of lgp to Lysosomes

We used a variety of independent approaches to determine whether lgp's can take a direct route from the TGN to lysosomes or must make obligatory passage through the plasma membrane. First, although not definitive, the fact that at steady state little wild-type lgp120 was found on the surface suggested that the plasma membrane was not a major intermediate on the pathway to lysosomes. Virtually no surface lgp was detected in NRK cells or in CHO transfectants expressing low levels of lgp. Even in high expressing transfectants, only a small fraction (estimated at ~1.5%) of the total rat lgp120 was found on the plasma membrane. In contrast, far greater fractions of lgp120G→A7 and lgp120Y→C8 localized at the plasma membrane of even low expressing cells (estimated at ~5.4 and 39%, respectively) (Table I).

Since wild-type lgp120 and lgp120G→A7 were internalized to the same extents and at comparable rates, equal amounts of ¹²⁵I-anti-lgp120 IgG should have been taken up at 37°C if both passed through the cell surface to similar extents. However, no antibody uptake over background was measured in NRK cells or low expressing wild-type transfectants (Table I). Specific antibody internalization was detected in cells expressing high levels of the wild-type protein. However, the amount of antibody internalized was less than that internalized by cells expressing a two- to threefold lower level of lgp120G→A7. When normalized for expression levels, cells overexpressing wild-type lgp120 were only 30% as efficient at internalizing externally added anti-lgp120 antibody as cells expressing the lgp120G→A7 mutant, in spite of the fact that both cell lines internalized cell surface lgp120 at comparable rates (Table I). This result suggests that the majority of wild-type lgp120 never reaches the plasma membrane, even in overexpressing cells.

Finally, we were able to directly determine the fraction of newly synthesized lgp120 appearing at the cell surface after pulse labeling. If all lgp's were transported to lysosomes by endocytosis after insertion in the plasma membrane, we would have expected a substantial fraction of pulse labeled lgp120 to be transiently accessible to either of the two cell surface labeling procedures used to detect surface appearance. This proved not to be the case. In NRK cells, only a very small cohort (<2%) of endogenous lgp120 molecules

reached the plasma membrane after leaving the Golgi complex. A somewhat greater fraction was observed in transfected CHO cells, ranging from ~15% of the total in cells expressing low levels of rat Igpl20 to ~25% in cells expressing higher amounts of the protein (Table I). Moreover, much of the labeled Igpl20 reaching the surface in high expressing cells was not rapidly cleared from the plasma membrane, suggesting that this pool of Igpl20 was not efficiently transferred to lysosomes. The slow clearance from the plasma membrane is difficult to reconcile with previous observations in NRK and J774 cells that Igpl20 is transported from the Golgi complex to lysosomes with a $t_{1/2}$ of <30 min (Green et al., 1987). Moreover, since even in the high expressing cells only a small fraction of the total Igpl20 synthesized ever appeared on the plasma membrane, it was unlikely that the cell surface served as an obligatory intermediate on the pathway to lysosomes.

The significance of these results was emphasized by the behavior of the two Igpl20 cytoplasmic domain mutants, Igpl20G→A7 and Igpl20Y→C8. Almost all of the newly synthesized Igpl in cells expressing the tyrosine mutant appeared on the surface within 30 min after pulse labeling (Table I). As shown previously (Williams and Fukuda, 1990), we found that this mutant accumulates on the plasma membrane and is incapable of rapid endocytosis. More importantly, a similarly large fraction of newly synthesized Igpl20G→A7 mutant (~70%) was also detected on the plasma membrane. Since the Igpl20G→A7 was internalized at an efficiency comparable to wild-type Igpl20, its increased appearance on the cell surface could not be explained by a markedly decreased rate of endocytosis. Besides, as was found for wild-type Igpl20 in overexpressing cells, much of the Igpl20G→A7 mutant was not rapidly cleared from the cell surface. These results suggest that Igpl's on the cell surface may not always be rapidly transported to lysosomes. Instead, especially when expressed at high levels, plasma membrane Igpl20 may recycle several times as shown for cell surface LAP (Braun et al., 1989).

Taken together, these experiments strongly suggest that the majority of newly synthesized Igpl20 molecules reach their final destinations without requiring prior insertion into the plasma membrane. This conclusion is further supported by our finding that in transfected MDCK cells only a small fraction of wild-type Igpl20 localized at the basolateral surface from which it was efficiently internalized (Hunziker et al., 1991). To a first approximation, this conclusion is different from that reached for the transport of an endogenous lysosomal protein in MDCK cells (Nabi et al., 1991). A substantial fraction of this protein, possibly an Igpl-B (Nabi, I., personal communication), was found to appear at the basolateral surface of MDCK cells before arrival in lysosomes. While this difference might be explained by differences in cell type or protein, it seems more likely to reflect the fact that these experiments detected surface appearance using antibody added at 37°C as opposed to 0°C. Thus, as the authors pointed out, their experiments could not quantitatively distinguish between surface appearance and insertion of newly synthesized Igpl into endosomes. In any event, final proof of actual pathway taken by Igpl20 must await identification of the actual carrier vesicles involved in its transport from the TGN.

Transport to Lysosomes May Involve a Saturable Intracellular Sorting Element

The correlation between expression level and cell surface appearance of Igpl20, combined with the missorting of endogenous hamster Igpl-B in transfectants expressing high concentrations of Igpl20, suggest that existence of an intracellular mechanism of limited capacity that is responsible for the proper targeting of Igpl molecules. While the nature of this putative sorting element is unknown, one attractive possibility is that it reflects the necessity for newly synthesized Igpl20 to enter a specific population of TGN-derived vesicles that target transport to endosomes and lysosomes. Conceivably, these vesicles may be the clathrin-coated vesicles thought to mediate the transport of MPR-bound lysosomal enzymes from the TGN to endosomes (Kornfeld and Mellman, 1989). Thus, in the presence of excess Igpl20 in overproducing cells, an increasing fraction of transfected and endogenous Igpl's would be transported to the plasma membrane as a consequence of increased competition for a limited number of sorting sites.

These results are analogous, but not identical to, earlier observations in yeast cells in which the eightfold overexpression of the vacuolar protease carboxypeptidase Y led to secretion of up to 50% of the newly synthesized enzyme (Stevens et al., 1986). However, carboxypeptidase Y overexpression did not lead to the missorting of other vacuole proteases. Since in CHO cells, overexpression of a transfected Igpl-A was associated with the plasma membrane appearance of both the transfected protein and an endogenous Igpl-B, it is conceivable that both classes of closely related Igpl molecules compete for a single sorting element. All Igpl-A and Igpl-B molecules sequenced thus far contain a glycine-tyrosine motif in their cytoplasmic domains (Kornfeld and Mellman, 1989). It is now apparent that both of these residues play a role in determining the proper intracellular targeting of newly synthesized Igpl molecules.

Cytoplasmic Tails and Sorting Signals

While a tyrosine in the cytoplasmic domain of Igpl20 is clearly important for lysosomal targeting, it is not yet clear why this is the case. The majority of newly synthesized Igpl20 molecules did not appear to be inserted into the plasma membrane before reaching lysosomes. Therefore, it is unlikely that tyrosine mutants are unable to be delivered to lysosomes solely because they cannot be rapidly internalized—in spite of the fact that the tyrosine is also required for rapid internalization. Instead, it is more likely that the tyrosine is involved in specifying an intracellular sorting event.

By analogy to the extensively studied role of cytoplasmic domain tyrosine residues in the localization of plasma membrane receptors at clathrin-coated pits (Davis et al., 1986; Jing et al., 1990; Lobel et al., 1989), it is conceivable that the Igpl20 cytoplasmic tail tyrosine performs a similar function in the TGN, allowing newly synthesized proteins to accumulate along with MPR at clathrin-coated buds which yield coated vesicles targeted for delivery to endosomes (Kornfeld and Mellman, 1989). Thus far, there is no direct evidence that Igpl's exit the TGN via clathrin-coated vesicles. Nor is it clear whether coated buds in the Golgi complex even recognize tyrosine-containing cytoplasmic domain de-

terminants. Indeed, *in vitro* binding studies suggest that adaptor proteins in Golgi-derived coated vesicles, thought to interact with receptor cytoplasmic domains, do not interact with the tyrosine-containing portions of the MPR cytoplasmic tail (Glickman et al., 1989; Pearse, 1988). The conserved glycine-tyrosine motif characteristic of Igpl20 has not yet been examined for adaptor protein interaction *in vitro*, nor is it clear that the same mechanism will apply in intact cells. Alternatively, the glycine-tyrosine-containing Igpl20 cytoplasmic domain might indirectly specify entry into TGN coated buds, or may reflect the formation of a nonclathrin-coated vesicle (Duden et al., 1991; Serafini et al., 1991) which may mediate lysosomal transport by an as yet uncharacterized pathway.

It is apparent, however, that the Igpl20 cytoplasmic domain tyrosine is involved in at least one additional biosynthetic sorting event. In MDCK cells transfected with the Igpl20G→A7 mutant, a large fraction of newly synthesized molecules was found to appear on the basolateral surface (Hunziker et al., 1991). Mutation of the cytoplasmic domain tyrosine completely reversed the polarity of surface expression resulting in the transport of the Igpl20Y→C8 mutant to the apical plasma membrane. Whether basolateral transport reflects inclusion of Igpl20 into TGN-derived clathrin-coated vesicles in MDCK cells is unknown, but it is clear that sorting of newly synthesized molecules in the Golgi complex is dependent on the Igpl20 cytoplasmic domain tyrosine. Conceivably, the mechanism leading to basolateral insertion in polarized cells, as well as to transport to lysosomes, may depend on common elements. If, in either polarized or nonpolarized cells, Igpl20 exits the TGN in clathrin-coated vesicles, then their possible role in the transport of even plasma membrane receptors containing coated pit localization domains should be considered.

We thank Michael Hull for expert assistance with the mutagenesis and Henry Tan for excellent photographic work. We are grateful to Susan Stuart (University of California at San Francisco) for providing the pFCMneo plasmid vector, to Randall Kaufman (Genetics Institute, Cambridge, MA) for the pMT21 plasmid vector, and to Suzanne Pfeffer (Stanford University, Stanford, CA) for kindly returning large amounts of purified E9a IgG made from a hybridoma cell line we provided. We are indebted to the Mellman/Helenius laboratories for helpful discussions.

This research was supported by grants from the National Institutes of Health and Boehringer-Ingelheim Pharmaceuticals, Inc. to I. Mellman. C. Harter was a recipient of fellowships from the Swiss National Science Foundation and the European Molecular Biology Organization.

Received for publication 25 October 1991 and in revised form 23 January 1992.

References

- Braun, M., A. Waheed, and K. von Figura. 1989. Lysosomal acid phosphatase is transported to lysosomes via the cell surface. *EMBO (Eur. Mol. Biol. Organ.) J.* 8:3633-3640.
- Bretscher, M. S., and R. Lutter. 1988. A new method for detecting endocytosed proteins. *EMBO (Eur. Mol. Biol. Organ.) J.* 7:4087-4092.
- Cha, Y., S. M. Holland, and J. T. August. 1990. The cDNA sequence of mouse LAMP-2. *J. Biol. Chem.* 265:5008-5013.
- Chen, J., Y. Cha, K. U. Yukesl, R. W. Gracy, and J. T. August. 1988. Isolation and sequencing of a cDNA clone encoding lysosomal membrane glycoprotein mouse LAMP-1. *J. Biol. Chem.* 263:8754-8758.
- Davis, C. G., M. Lehrman, D. Russel, R. G. W. Anderson, M. Brown, and G. L. Goldstein. 1986. The J. D. mutation in familial hypercholesterolemia: amino acid substitution in the cytoplasmic domain impedes internalization of LDL receptors. *Cell.* 45:15-24.
- D'Souza, M. P., and J. T. August. 1986. A kinetic analysis of biosynthesis and localization of a lysosome-associated membrane glycoprotein. *Arch. Biochem. Biophys.* 249:522-532.
- Duden, R., G. Griffiths, R. Frank, P. Argos, and T. E. Kreis. 1991. β -COP, a 110-kD protein associated with non-clathrin-coated vesicles and the Golgi complex, shows homology to β -adaptin. *Cell.* 64:649-665.
- Fambrough, D. M., K. Takeyasu, J. Lippincott-Schwartz, N. Siegel, and D. Somerville. 1988. Structure of LEP100, a glycoprotein that shuttles between lysosomes and the plasma membrane, deduced from the nucleotide sequence of the encoding cDNA. *J. Cell Biol.* 96:61-67.
- Furuno, K., T. Ishikawa, K. Akasaki, S. Yano, Y. Tanaka, Y. Yamaguchi, H. Tsuji, M. Himeno, and K. Kato. 1989a. Morphological localization of a major lysosomal membrane glycoprotein in the endocytic membrane system. *J. Biochem. (Tokyo).* 106:708-716.
- Furuno, K., S. Yano, K. Akasaki, Y. Tanaka, Y. Yamaguchi, H. Tsuji, M. Himeno, and K. Kato. 1989b. Biochemical analysis of the movement of a major lysosomal membrane glycoprotein in the endocytic membrane system. *J. Biochem. (Tokyo).* 106:717-722.
- Glickman, J. N., E. Conibar, and B. M. F. Pearse. 1989. Specificity of binding of clathrin adaptors to signals on the mannose 6-phosphate/insulin-like growth factor II receptor. *EMBO (Eur. Mol. Biol. Organ.) J.* 8:1041-1047.
- Granger, B. L., S. A. Green, C. A. Gabel, C. L. Howe, I. Mellman, and A. Helenius. 1990. Characterization and cloning of Igpl10, a lysosomal membrane glycoprotein from mouse and rat cells. *J. Biol. Chem.* 265:12036-12043.
- Green, S. A., K.-P. Zimmer, G. Griffiths, and I. Mellman. 1987. Kinetics of intracellular transport and sorting of lysosomal membrane and plasma membrane proteins. *J. Cell Biol.* 105:1227-1240.
- Himeno, M., Y. Noguchi, H. Sasaki, Y. Tanaka, K. Furuno, A. Kono, Y. Sakaki, and K. Kato. 1989. Isolation and sequencing of a cDNA clone encoding 107-kD sialoglycoprotein in rat liver lysosomal membranes. *FEBS (Fed. Eur. Biochem. Soc.) Lett.* 244:351-356.
- Horwich, A. L., W. A. Fenton, F. A. Firgaira, F. E. Fox, D. Kolansky, and I. S. Mellman. 1985. Expression of amplified DNA sequences for ornithine transcarbamylase in HeLa cells: arginine residues may be required for mitochondrial import of enzyme precursor. *J. Cell Biol.* 100:1515-1521.
- Howe, C. L., B. L. Granger, M. Hull, S. A. Green, C. A. Gabel, A. Helenius, and I. Mellman. 1988. Derived protein sequence, oligosaccharides, and membrane insertion of the 120-kD lysosomal membrane glycoprotein (Igpl20): identification of a highly conserved family of lysosomal membrane glycoproteins. *Proc. Natl. Acad. Sci. USA.* 85:7577-7581.
- Hunziker, W., C. Harter, K. Matter, and I. Mellman. 1991. Basolateral sorting in MDCK cells requires a distinct cytoplasmic domain determinant. *Cell.* 66:907-920.
- Jing, S., T. Spencer, K. Miller, C. Hopkins, and I. S. Trowbridge. 1990. Role of the human transferrin receptor cytoplasmic domain in endocytosis: localization of a specific signal sequence for internalization. *J. Cell Biol.* 110:2283-2294.
- Kaufman, R. J. 1990a. Vectors used for expression in mammalian cells. *Methods Enzymol.* 185:487-511.
- Kaufman, R. J. 1990b. Selection and coamplification of heterologous genes in mammalian cells. *Methods Enzymol.* 185:537-566.
- Kornfeld, S., and I. Mellman. 1989. The biogenesis of lysosomes. *Annu. Rev. Cell Biol.* 5:483-525.
- Ktistakis, N. T., D. Thomas, and M. G. Roth. 1990. Characteristics of the tyrosine recognition signal for internalization of transmembrane surface glycoproteins. *J. Cell Biol.* 111:1393-1407.
- Kunkel, T. A. 1985. Rapid and efficient site-directed mutagenesis without phenotypic selection. *Proc. Natl. Acad. Sci. USA.* 82:488-492.
- Lewis, V., S. A. Green, M. Marsh, P. Vihko, A. Helenius, and I. Mellman. 1985. Glycoproteins of the lysosomal membrane. *J. Cell Biol.* 100:1839-1847.
- Lippincott-Schwartz, J., and D. M. Fambrough. 1986. Lysosomal membrane dynamics: structure and interorganellar movement of a major lysosomal membrane glycoprotein. *J. Cell Biol.* 102:1593-1605.
- Lobel, P., K. Fujimoto, R. D. Ye, G. Griffiths, and S. Kornfeld. 1989. Mutations in the cytoplasmic domain of the 275-kD mannose 6-phosphate receptor differentially alter lysosomal enzyme sorting and endocytosis. *Cell.* 57:787-796.
- Mane, S. M., L. Marzella, D. F. Bainton, V. K. Holt, T. Cha, K. Hildreth, and J. T. August. 1989. Purification and characterization of human lysosomal membrane glycoproteins. *Arch. Biochem. Biophys.* 268:360-378.
- McLean, I. W., and P. K. Nakane. 1974. Periodate-lysine-paraformaldehyde fixative. A new fixative for immunoelectron microscopy. *J. Histochem. Cytochem.* 22:1077-1083.
- Miettinen, H. M., J. K. Rose, and I. Mellman. 1989. Fc receptor isoforms exhibit distinct abilities for coated pit localization as a result of cytoplasmic domain heterogeneity. *Cell.* 58:317-327.
- Nabi, I. R., A. Le Bivic, D. Fambrough, and E. Rodriguez-Boulan. 1991. An endogenous MDCK lysosomal membrane glycoprotein is targeted basolaterally before delivery to lysosomes. *J. Cell Biol.* 115:1573-1584.
- Noguchi, Y., M. Himeno, H. Sasaki, Y. Tanaka, A. Kono, Y. Sakaki, and K. Kato. 1989. Isolation and sequencing of a cDNA clone encoding 96-kD sialoglycoprotein in rat liver lysosomal membranes. *Biochem. Biophys. Res. Commun.* 164:1113-1120.
- Pearse, B. M. F. 1988. Receptors compete for adaptors found in plasma mem-

- brane coated pits. *EMBO (Eur. Mol. Biol. Organ.) J.* 7:3331-3336.
- Peters, C., M. Braun, B. Weber, M. Wendland, B. Schmidt, R. Pohlmann, A. Waheed, and K. von Figura. 1990. Targeting of a lysosomal membrane protein: a tyrosine-containing endocytosis signal in the cytoplasmic tail of lysosomal acid phosphatase is necessary and sufficient for targeting to lysosomes. *EMBO (Eur. Mol. Biol. Organ.) J.* 9:3497-3506.
- Sanger, F., S. Nicklen, and A. R. Coulson. 1977. DNA sequencing with chain terminating inhibitors. *Proc. Natl. Acad. Sci. USA.* 74:5463-5467.
- Serafini, T., G. Stenbeck, A. Brecht, F. Lottspeich, L. Orci, J. E. Rothman, and F. T. Wieland. 1991. A coat subunit of Golgi-derived non-clathrin-coated vesicles with homology to the clathrin-coated vesicle coat protein β -adaptin. *Nature (Lond.)* 349:215-220.
- Stevens, T. H., J. H. Rothman, G. S. Payne, and R. Schekman. 1986. Gene dosage-dependent secretion of yeast vacuolar carboxypeptidase Y. *J. Cell Biol.* 102:1551-1557.
- Viitala, J., S. R. Carlsson, P. D. Siebert, and M. Fukuda. 1988. Molecular cloning of cDNAs encoding lamp A, a human lysosomal membrane glycoprotein with apparent $M_r = 120,000$. *Proc. Natl. Acad. Sci. USA.* 85:3743-3747.
- Wigler, M., A. Pellicer, S. Silverstein, R. Axel, G. Urlaub, and L. Chasin. 1979. DNA-mediated transfer of the adenine phosphoribosyltransferase locus into mammalian cells. *Proc. Natl. Acad. Sci. USA.* 76:1373-1376.
- Williams, M. A., and M. Fukuda. 1990. Accumulation of membrane glycoproteins in lysosomes requires a tyrosine residue at a particular position in the cytoplasmic tail. *J. Cell Biol.* 111:955-966.